PNAS
www.pnas.org

Supplementary Information for:

**Agonist-induced formation of unproductive receptor-$G_{12}$ complexes**

Najeah Okashah, Shane C. Wright, Kouki Kawakami, Signe Mathiasen, Joris Zhou, Sumin Lu, Jonathan A. Javitch, Asuka Inoue, Michel Bouvier and Nevin A. Lambert

Correspondence to: Nevin A. Lambert
Email: nelambert@augusta.edu

**This PDF file includes:**

Figures S1 to S12
Table S1



www.pnas.org/cgi/doi/10.1073/pnas.2003787117

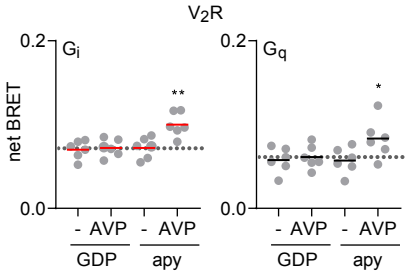


**Figure S1.** $V_2R$ forms GDP-sensitive agonist-induced complexes with $G_i$ and $G_q$ heterotrimers. BRET between $V_2R$-Rluc8 and $G\alpha\beta\gamma$-Venus in the presence or absence of arginine vasopressin (AVP; 1 μM), and the presence or absence of GDP. When GDP was absent apyrase (apy) was added to remove residual nucleotides. These results are consistent with activation of $G_i$ and $G_q$ heterotrimers by $V_2R$ that may or may not lead to signaling, as cooperativity between agonist and nucleotide binding is only one requirement for efficient G protein activation; physiological activation of $G_i$ heterotrimers by $V_2R$ will require confirmation. In each panel the broken gray line represents net BRET when agonist and GDP are both present, and solid lines represent the mean of the superimposed data points; $^{**}P<0.005$, $^{*}P<0.05$; one-way ANOVA (Sidak's test) compared to GDP + AVP; $n=6$.

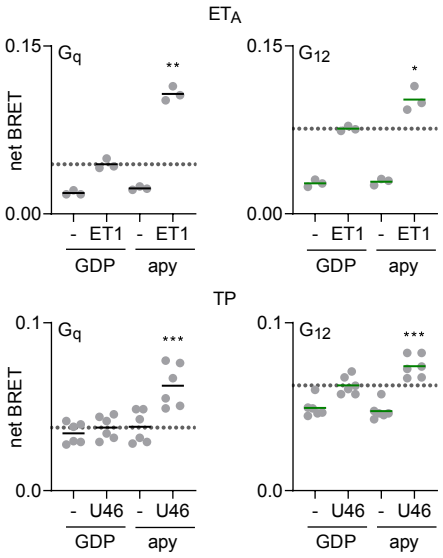


**Figure S2.** $ET_A$ and TP receptors form GDP-sensitive agonist-induced complexes with $G_q$ and $G_{12}$ heterotrimers. BRET between $ET_A$-Rluc8 (*top*) and TP-Rluc8 (*bottom*) and $G\alpha\beta\gamma$-Venus in the presence or absence of the agonists endothelin-1 (ET1; 100 nM) and U-46619 (U46; 10 μM), in the presence and absence of GDP. For both of these receptors agonist-induced BRET to $G_q$ (*left*) and $G_{12}$ (*right*) heterotrimers was enhanced when GDP was absent. In each panel the broken gray line represents net BRET when agonist and GDP are both present, and solid lines represent the mean of the superimposed data points; **P*<0.05, ***P*<0.005, ****P*<0.0005; one-way ANOVA (Sidak's test) compared to GDP + agonist; *n*=3-6.

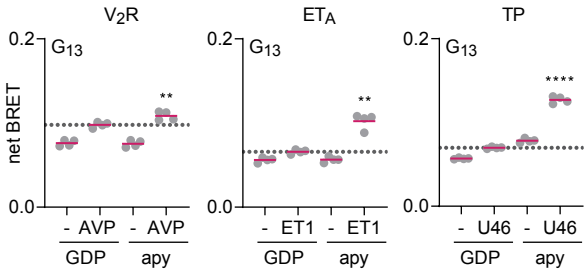


**Figure S3.** $V_2R$, $ET_A$ and TP receptors form GDP-sensitive agonist-induced complexes with $G_{13}$ heterotrimers. BRET between $V_2R$-Rluc8, $ET_A$-Rluc8 and TP-Rluc8 and $G\alpha\beta\gamma$-Venus in the presence or absence of the agonists arginine vasopressin (AVP; 1 μM), endothelin-1 (ET1; 100 nM) and U-46619 (U46; 10 μM), in the presence and absence of GDP. When GDP was absent apyrase (apy) was added to remove residual nucleotides. In each panel the broken gray line represents net BRET when agonist and GDP are both present, and solid lines represent the mean of the superimposed data points; $^{**}P<0.005$, $^{****}P<0.0001$; one-way ANOVA (Sidak's test) compared to GDP + agonist; $n=4$.

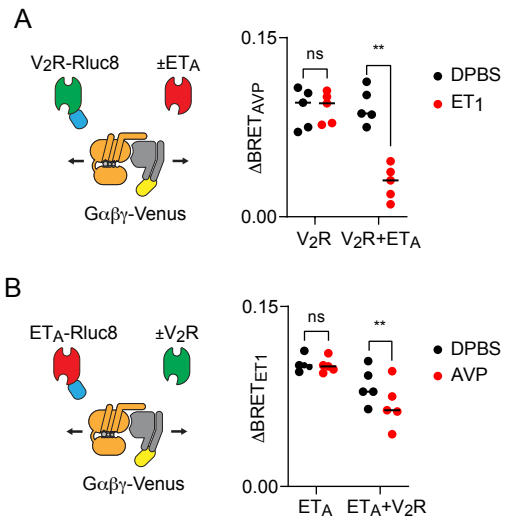


**Figure S4.** $V_2R$ and $ET_A$ receptors compete for a common pool of $G_{12}$ heterotrimers in intact cells. (*A*) Agonist-induced (AVP; 1 μM) BRET between $V_2R$-Rluc8 and $G\alpha_{12}\beta\gamma$-Venus is significantly inhibited when unlabeled $ET_A$ receptors are coexpressed and activated (ET1; 100 nM); n.s., not significant (*P*=0.92); ***P*<0.05; one-way ANOVA (Sidak's test); *n*=5. (*B*) Agonist-induced (ET1; 100 nM) BRET between $ET_A$-Rluc8 and $G\alpha_{12}\beta\gamma$-Venus is significantly inhibited when unlabeled $V_2R$ receptors are coexpressed and activated (AVP; 1 μM); n.s., not significant (*P*=0.71); ***P*<0.005; one-way ANOVA (Sidak's test); *n*=5. Data points represent the change in BRET (ΔBRET) in response to agonist.

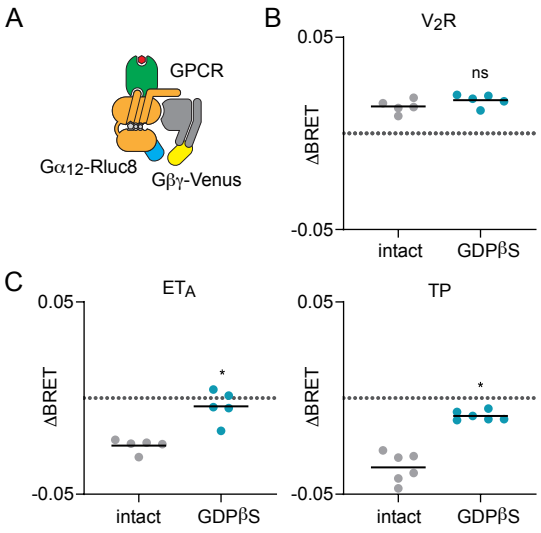


**Figure S5.** Active $V_2R$ receptors induce a conformational change in a $G_{12}$ BRET biosensor that does not require activation. (*A*) Unlabeled receptors were coexpressed with $G_{12}$-Rluc8 and Gβγ-Venus in intact cells, or in cells that were permeabilized in the presence of apyrase and GDPβS (10 μM) to prevent $G_{12}$ activation. (*B*) When $V_2R$ receptors were expressed AVP (1 μM) increased BRET between $G_{12}$-Rluc8 and Gβγ-Venus in intact cells. Similar responses were observed when $G_{12}$ activation was prevented in permeabilized cells. (*C*) When $ET_A$ and TP receptors were expressed ET1 (100 nM) and U46 (10 μM) decreased BRET between $G_{12}$-Rluc8 and Gβγ-Venus in intact cells. These responses were largely blocked when $G_{12}$ activation was prevented. Data points represent the change in BRET (ΔBRET) in response to agonist, and the broken gray line represents zero; n.s., not significant; **P*<0.005; unpaired t-test compared to intact cells; *n*=5-6. All datasets with the exception of $ET_A$ in the presence of GDPβS were significantly different from zero (*P*<0.005; one-sample t-test), indicating a significant positive or negative response to agonist.

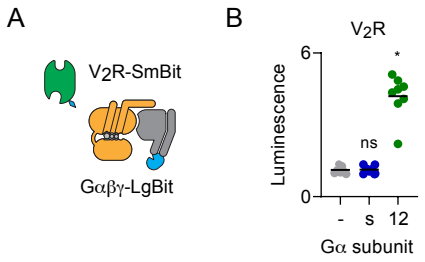


**Figure S6.** Luciferase complementation reports association of $V_2R$ and $G_{12}$ heterotrimers in intact cells. (*A*) $V_2R$ was fused to a small fragment (SmBit) of NanoLuc luciferase (Nluc) and $G\gamma_2$ subunits were fused to a large fragment (LgBit) of Nluc. (*B*) Activation of $V_2R$ with AVP (1μM) increases luciferase activity when $G\alpha_{12}$ is cotransfected, but not when $G\alpha_s$ or empty vector (-) is cotransfected. Data points represent luminescence normalized to vehicle-treated controls; $P<0.0001$; n.s., not significant compared to mock-transfected controls (-); one-way ANOVA (Dunnett's test); $n=8$.

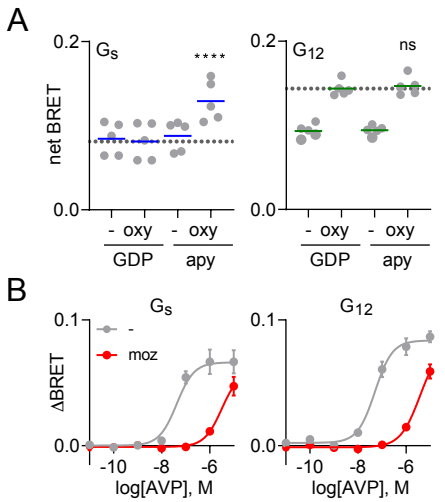


**Figure S7.** Oxytocin-bound $V_2R$ forms unproductive complexes with $G_{12}$ heterotrimers. (*A*) BRET between $V_2R$-Rluc8 and $G\alpha\beta\gamma$-Venus in the presence or absence of oxytocin (oxy; 1 μM), and the presence or absence of GDP. Oxytocin-induced BRET to $G_s$ (*left*) but not $G_{12}$ (*right*) heterotrimers was enhanced when GDP was absent. When GDP was absent apyrase (apy) was added to remove residual nucleotides. In each panel the broken gray line represents net BRET when agonist and GDP are both present, and solid lines represent the mean of the superimposed data points; ****$P$<0.0001; n.s., not significant ($P$=0.34); one-way ANOVA (Sidak's test) compared to GDP + oxytocin; $n$=5. (*B)* Addition of the $V_2R$ inverse agonist mozavaptan (moz; 1 μM) inhibits AVP-induced BRET between $V_2R$-Rluc8 and $G_s$ or $G_{12}$ heterotrimers in nucleotide-depleted cells (mean ± SEM; $n$=3).

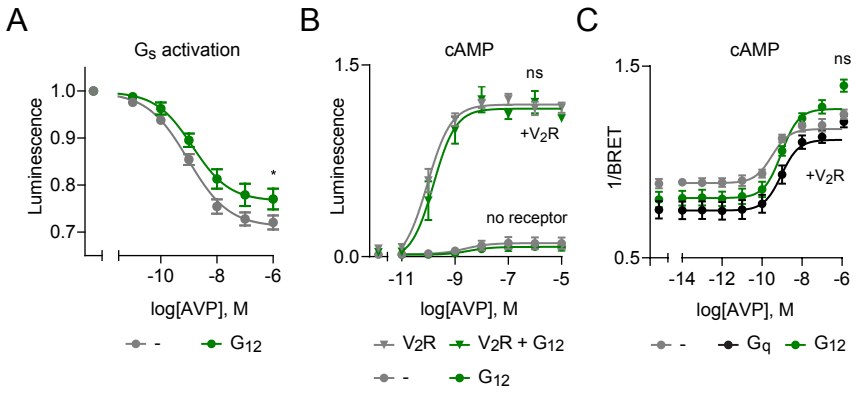


**Figure S8.** Overexpressing $G_{12}$ heterotrimers inhibits activation of $G_s$ heterotrimers, but not $V_2R$-mediated cyclic AMP (cAMP) accumulation. (*A*) Activation of a Nanobit $G_s$ activation sensor is inhibited when $G_{12}$ is overexpressed; mean ± SEM; *n*=4. (*B* and *C*) AVP-induced increases in cAMP were monitored using a Glosensor assay (*B*) and an EPAC-based cAMP sensor (*C*); mean ± SEM; *n*=3-6. Values in *B* and *C* were normalized to responses to forskolin (100 μM); **P*<0.05; n.s., not significant; paired t-test versus mock-transfected control (-) at 1 μM AVP.

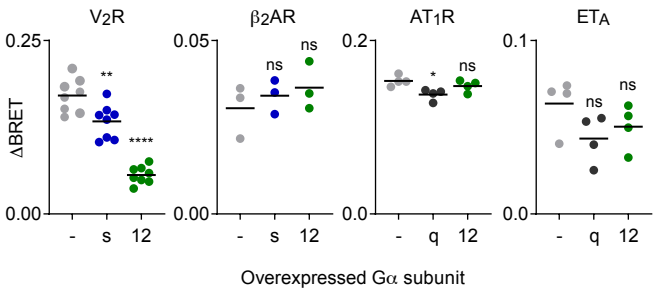


**Figure S9.** Overexpressing $G_{12}$ heterotrimers does not inhibit arrestin recruitment to $ET_A$, $\beta_2$ adrenergic, or angiotensin $AT_1$ receptors. Recruitment of β-arrestin2-Venus to $V_2$R-Rluc8 is inhibited when $G_{12}$ is overexpressed. A smaller inhibition is observed when $G_s$ is overexpressed. In contrast, β-arrestin2-Venus recruitment to $\beta_2$AR-Rluc8, $AT_1$R-Rluc8, and $ET_A$-Rluc8 is not inhibited by $G_{12}$ overexpression. Overexpression of cognate G proteins also did not inhibit arrestin recruitment, with the exception of $G_q$ heterotrimers and $AT_1$ receptors; ****$P$<0.0001; **$P$=0.004; *$P$=0.015; n.s., not significant compared to mock-transfected controls (-); one-way ANOVA (Dunnett's test); $n$=3-8. Data points represent the change in BRET (ΔBRET) in response to agonist stimulation. Agonists were AVP (1 μM), isoproterenol (10 μM), angiotensin II (1 μM), and ET1 (100 nM).

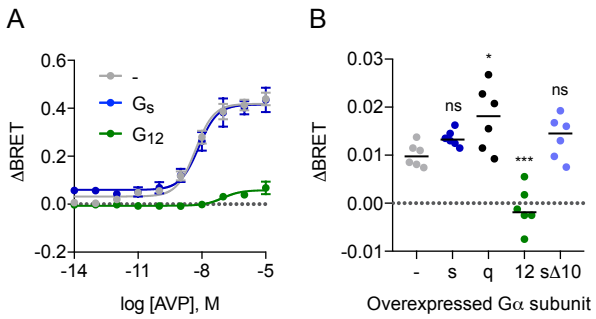


**Figure S10.** Overexpressing $G_{12}$ heterotrimers inhibits GRK2 recruitment to $V_2R$. (*A*) Overexpressing $G_{12}$ but not $G_s$ heterotrimers inhibits AVP-induced changes in bystander BRET between GRK2-RlucII D110A and the plasma membrane marker rGFP-CAAX (mean ± SEM; *n*=3-6). (*B*) Overexpressing $G_{12}$ but not $G_s$, $G_q$ or $G_s\Delta10$ heterotrimers inhibits AVP-induced BRET between $V_2R$-Rluc8 and GRK2-Venus-Kras R587Q, which was tethered to the plasma membrane with a CAAX motif and incorporated a mutation (R587Q) to prevent binding to $G\beta\gamma$ dimers; ***$P$<0.0005; *$P$<0.05; n.s., compared to mock-transfected controls (-); one-way ANOVA (Dunnett's test); *n*=6. $G_s\Delta10$ heterotrimers lacked ten amino acids at the C terminus of $G\alpha_s$, and therefore could not be activated by $V_2R$.

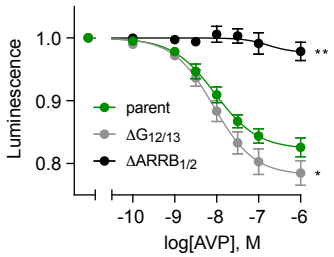


**Figure S11.** $V_2R$ internalization is enhanced in cells lacking $G_{12}$. Loss of cell surface luminescence due to internalization of HiBit-$V_2R$ was measured 30 minutes after addition of AVP. Cells were parental HEK 293 cells, 293 cells lacking both $G\alpha_{12}$ and $G\alpha_{13}$ subunits ($\Delta G_{12/13}$), or 293 cells lacking both $\beta$ -arrestin1 and $\beta$-arrestin2 ($\Delta ARRB_{1/2}$); $^{**}P<0.005$; $^{*}P<0.05$, compared to parental cells; one-way ANOVA (Dunnett's test); $n$=6.

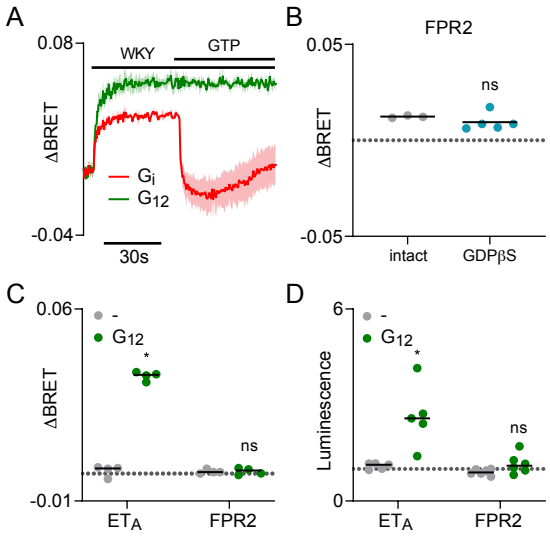


**Figure S12.** Active FPR2 receptors bind but do not activate $G_{12}$ heterotrimers. (*A*) Time course of BRET between FPR2-Rluc8 and Gαβγ-Venus in response to injection of 500 nM WKYMVm (WKY), followed by injection of 100 μM GTP in permeabilized cells treated with apyrase (mean ± SEM; *n*=3). (*B*) Stimulation of unlabeled FPR2 receptors with WKY (500 nM) increased BRET between $G_{12}$-Rluc8 and Gβγ-Venus in intact cells, and this response persisted in cells that were permeabilized in the presence of apyrase and GDPβS (10 μM) to prevent $G_{12}$ activation. Data points represent the change in BRET (ΔBRET) in response to WKY, and the broken gray line represents zero; n.s., not significant; unpaired t-test compared to intact cells; *n*=3-5. Both datasets were significantly different from zero (*P*<0.05; one-sample t-test), indicating a significant response to agonist. (*C*) Activation of FPR2 receptors with WKY (500 nM) has no effect on bystander BRET between p115RhoGEF-Rluc8 and the plasma membrane marker Venus-Kras when $G_{12}$ is expressed, whereas activation of $ET_A$ with ET1 (100 nM) increases this signal. Data points represent the change in bystander BRET (ΔBRET) in response to agonist, and the broken gray line represents zero. (*D*) Activation of FPR2 fails to activate the serum response element (SRE) when $G_{12}$ is expressed, whereas activation of $ET_A$ increases SRE-driven gene expression. Data points represent luminescence normalized to vehicle-treated controls, and the broken gray line represents one (no change); **P*<0.05; n.s., not significant; paired t-test compared to mock-transfected control (-); *n*=3-5.

**Table S1.** Receptors and agonists used and GDP resistance ($R_{GDP}$) observed in Figure 6. All receptors were human.

| Receptor-gene | $G_s$ $R_{GDP}$ | $G_i$ $R_{GDP}$ | $G_q$ $R_{GDP}$ | $G_{12}$ $R_{GDP}$ | ligand | concentration |
|---|---|---|---|---|---|---|
| $\beta_2$AR-*ADRB2* | 0.060 | | | | norepinephrine | 100 μM |
| $V_2$R-*AVPR2* | -0.005 | | | 1.019 | AVP | 1 μM |
| $H_2$R-*HRH2* | 0.208 | | | | amthamine | 100 μM |
| $D_1$R-*DRD1* | 0.231 | | | | dopamine | 100 μM |
| $\alpha_2$AR-*ADRA2A* | | 0.218 | | | norepinephrine | 100 μM |
| $M_4$R-*CHRM4* | | 0.089 | | | acetylcholine | 500 μM |
| $A_1$R-*ADORA1* | | 0.486 | | | adenosine | 100 μM |
| $D_2$R-*DRD2* | | 0.115 | | | dopamine | 100 μM |
| MOR-*OPRM1* | | 0.159 | | | DAMGO | 10 μM |
| FPR2-*FPR2/ALX* | | 0.294 | | 0.918 | WKYMVm | 500 nM |
| FPR1 | | 0.256 | | 0.964 | WKYMVm | 500 nM |
| smoothened-*Smo* | | 0.186 | | 1.012 | cyclopamine | 10 μM |
| $AT_1$R-*AGTR1* | | | 0.168 | | angiotensin II | 1 μM |
| $M_3$R-*CHRM3* | | | 0.086 | | acetylcholine | 500 μM |
| $H_1$R-*HRH1* | | | 0.107 | | histamine | 100 μM |
| $ET_A$R-*EDNRA* | | 0.232 | 0.290 | 0.700 | endothelin-1 | 100 nM |
| $ET_B$R-*EDNRB* | | 0.250 | 0.206 | 0.791 | endothelin-1 | 100 nM |
| TP-*TBXA2R* | | | 0.121 | 0.542 | U46619 | 10 μM |
| P2RY10-*P2RY10* | | 0.141 | | 0.099 | lyso PS 18:1 | 10 μM |
| GPR35-*GPR35* | | | | 0.308 | zaprinast | 10 μM |